PAPER

The time and frequency standard system for FAST receivers

The time and frequency standard system for FAST receivers

Kai Zhu (朱凯)[1], Jin Fan (范瑾)[1], Kun Liang[2], Wei Tang[1], Zhi-Sheng Gao[1], Yan Zhu[1], Yi Feng[1],
Wei-Wei Zhu[1], Lei Qian[1], You-Ling Yue[1], Jin-You Song[1], Xiang-Wei Shi[1], Xing-Yi Wang[1], Ming-Lei Guo[1],
Hang Zhang[1], Heng-Qian Gan[1], Hong-Fei Liu[1], Cheng-Jin Jin[1] and Peng Jiang[1]

[1] National Astronomical Observatories, Chinese Academy of Sciences, Beijing 100101, China; *jfan@bao.ac.cn*
[2] National Institute of Metrology, Beijing 100013, China

Abstract This paper reports on the time and frequency standard system for the Five-hundred meter Aperture Spherical radio Telescope (FAST), including the system design, stability measurements and pulsar timing observations. The stability and drift rate of the frequency standard are calculated using 1-year monitoring data. The UTC-NIM Disciplined Oscillator (NIMDO) system improves the system time accuracy and stability to the level of 5 ns. Pulsar timing observations were carried out for several months. The weighted RMS of timing residuals reaches the level of less than 3.0 μs.

Key words: FAST: radio telescope — time frequency standard — NIMDO:UTC-NIM

1 INTRODUCTION

The time and frequency standard system is necessary for modern radio telescopes. The frequency standard provides stable 5 MHz and 10 MHz sinusoidal signals to receivers, which are then synthesized to different frequencies required for frequency mixing or implemented as circuits in clock signals. On the other hand, the time standard provides accurate Coordinated Universal Time (UTC) for the receiver system. For some astronomy observations like pulsar timing and very long baseline interferometry (VLBI) observations, the time frequency accuracy and stability are very important and sometimes crucial to produce scientifically usable data.

Five-hundred-meter Aperture Spherical radio Telescope (FAST) is the largest single dish radio telescope in the world (Nan et al. 2011; Li & Pan 2016). It is located in Guizhou Province China. The 1st stage operating frequency band of FAST is 70 MHz–3 GHz. The key science goals include observations of the 21 cm HI line, pulsars, radio continuum, recombination lines, molecular spectral lines, VLBI, etc.

In the following, we will first provide an overview of the design of the time frequency standard system for FAST receivers. Then we will showcase long-term measurement

results of the frequency standard. The frequency stability and drift rate are calculated. The UTC-NIM Disciplined Oscillator (NIMDO), the core component of which is a high-stability local oscillator controlled by UTC (NIM) in near real time, was incorporated as an upgrade to the time frequency source. As an application and verification, we tested the accuracy of the time frequency standards through pulsar timing observations over several months.

2 SYSTEM DESIGN

Among the key science goals of FAST, VLBI and pulsar timing require very high time accuracy and long term time frequency stability from the time frequency sources.

For VLBI observations, different stations need to be synchronized accurately to avoid a time-consuming fringe search. The VLBI coherence function is defined as

$$C(T) = \frac{1}{T} \left| \int_0^T \exp(j\phi(t)) \, dt \right|, \tag{1}$$

where T is an arbitrary integration time, and $\phi(t)$ is the phase difference between the two stations forming the interferometer, caused primarily by frequency standards and atmospheric phase noises. The root-mean-square (RMS) value of $C(T)$ is a monotonically decreasing function of time T with the range 1 to 0, and a function of the interfer-

Table 1 EVN Central Frequencies at Low Frequencies

No	Waveband	Default central frequency
1	18 cm	1664 MHz
2	13 cm	2268 MHz
3	6 cm	4992 MHz
4	5 cm	6668 MHz (Methanol), 6030 MHz (OH)

Table 2 MHM2010 Hydrogen Maser Stability

No	Time Scale	ADEV
1	1 s	1.5×10^{-13}
2	10 s	2.0×10^{-14}
3	100 s	5.0×10^{-15}
4	1000 s	2.0×10^{-15}
5	10 000 s	1.5×10^{-15}
6	long term	$< 2 \times 10^{-16}$ per day

ometer phase difference $\phi(t)$ (Thompson & Moran 1989; Rogers & Moran 1981).

The RMS value of the phase difference ϕ in a period of time τ is approximately proportional to the Allan Standard Deviation (ADEV) σ_y, which represents the frequency stability of a signal

$$< \delta(\phi)^2 >_\tau^{1/2} \simeq 2\pi\nu_0\tau\sigma_y \,, \tag{2}$$

where $<>$ denotes the expectation value and ν_0 is the observing frequency.

The high frequency stability required for interferometer signals must be maintained during the observation. For short-term observations of a few minutes in which white phase noise dominates, as a rule of thumb, the ADEV of signals as well as the stability of frequency standards needs to be better than

$$\sigma_y = \frac{\sqrt{-6\ln\beta}}{2\pi\nu_0\tau_c} \,, \tag{3}$$

where β is the relative coherence amplitude, defined as the RMS value of the coherence $C(T)$, ranging from 1 to 0. τ_c is the coherence time, which is defined as the value of τ for which β drops to some specified value (Thompson & Moran 1989).

We adopt the European VLBI Network (EVN) working frequencies below 7 GHz as the operating frequencies for FAST VLBI observations, which are listed in Table 1.

As a typical example of VLBI observations, we choose $\beta = 0.9$, $\nu_0 = 2.268$ GHz and $\tau_c = 500$ s, thus the ADEV of the frequency standard should be lower than 1.0×10^{-13}.

On the other hand, for pulsar observations and dedispersion, the time accuracy must be better than 50 ns.

The flowchart of the time frequency standard system is displayed in Figure 1. Standard time signals are generated from GPS time servers, in the form of Pulse Per Second (PPS), the standard deviation of offset of which with respect to UTC is lower than 15 ns. The time standard contains two GPS time servers, one CNS Clock II time server and one Symmetricom SyncServer S650. Backend computers are synced to GPS time servers through network time protocol (NTP). The NTP offset is less than 5 ms in the local network utilized for FAST.

For the frequency standard, different kinds of high stability frequency sources have been considered, including a hydrogen maser, cesium clock, Rb clock, etc. So far, two frequency sources have been installed on the site. The major signal source is a Symmetricom MHM2010 Hydrogen Maser, which can provide high stability 5 MHz, 10 MHz and 100 MHz sinusoid signals. The ADEV at different time scales for the hydrogen maser signal is expressed in Table 2[1] (Wiley 2008). The secondary frequency standard is an SRS725 Rb Clock, which is prepared for emergency conditions.

A Symmetricom TSC4091 auto switch RF distributor is used as the first stage for standard frequency signal distribution. The A/B port of TSC4091 is connected to the hydrogen maser and Rb clock separately, so that the standard frequency source can be automatically switched to the secondary Rb standard in case that the primary hydrogen maser standard is down or needs maintenance.

A backup hydrogen maser will greatly improve the performance of the frequency standard system compared to the existing secondary Rb clock source. With the construction of a new clock room finished in the middle of 2019, a new hydrogen maser will be installed, and will provide better robustness for the frequency standard system.

3 MEASUREMENTS

3.1 Frequency Stability Measurement

The clock difference between the hydrogen maser and the GPS time server was measured by a frequency counter since the equipments were installed, and the clock difference data were gathered through ethernet by Grafana, an open source platform for time-series data monitoring and analysis. One year monitoring results from Sep 2017 to Sep 2018 are depicted in Figure 2. The hydrogen maser's long-term drift curve is plotted in Figure 3.

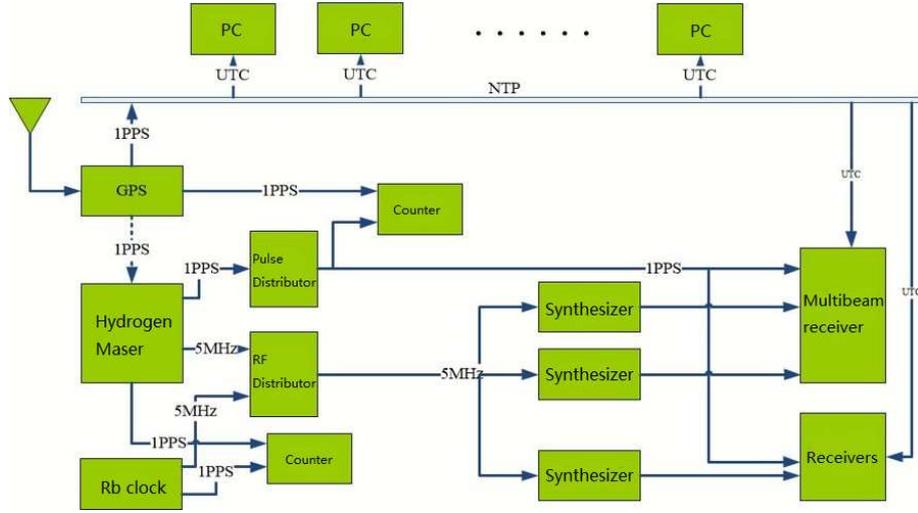[1] *https://www.microsemi.com/document-portal/ doc_download/133261-mhm-2010-datasheet*

**Fig. 1** Time frequency standard system flowchart.

Fig. 2 One year monitoring of GPS and hydrogen maser 1PPS clock difference from Sep 2017 to Sep 2018. The data were collected and plotted by Grafana, open source software for time series analysis and monitoring. The 1PPS difference data were sampled at the rate of 1 sample per minute, and smoothed every 6 hours. The *yellow line* represents the smoothed time difference between GPS and hydrogen maser 1PPS signal. The *light-blue line* signifies the derivative of the *yellow line*, though which the short-term fluctuations in the data can be easily found. The gaps and spikes in the derivative curve are due to the loss of some monitoring data, which were primarily caused by temporary electric power failure events.

The red solid line in Figure 3 is the fitted curve, which is quite consistent with the 1-year monitoring data represented by the green dotted line. From the monitoring process, the growth rate in the average hydrogen maser clock error rate is calculated, which is $68\,\mathrm{ns\,d^{-1}}$. The growth rate in clock error is caused by the frequency offset of the hydrogen maser with respect to the nominal standard frequency, thus the average fractional frequency offset can be calculated, which is $OFFSET_{\mathrm{hm}} = 7.87 \times 10^{-13}$.

The absolute frequency offset of the 5 MHz signal from the hydrogen maser is 3.935×10^{-6} Hz. From the s-lope of the clock error derivatives, the long term frequency drift of the hydrogen maser can be calculated. The fractional frequency drift rate is $DRIFT_{\mathrm{hm}} = 1.099 \times 10^{-16}\,\mathrm{d^{-1}}$.

The output frequency of the MHM2010 Hydrogen Maser was adjusted through the serial port and front panel after one year of monitoring. After adjustment, the time drift decreased to about $12\,\mathrm{ns\,d^{-1}}$, and correspondingly the relative frequency offset decreased to 1.39×10^{-13}. The maser adjustment operations need to be done carefully so as to not affect the physical working conditions of the instrument. If the working state of the maser is changed due
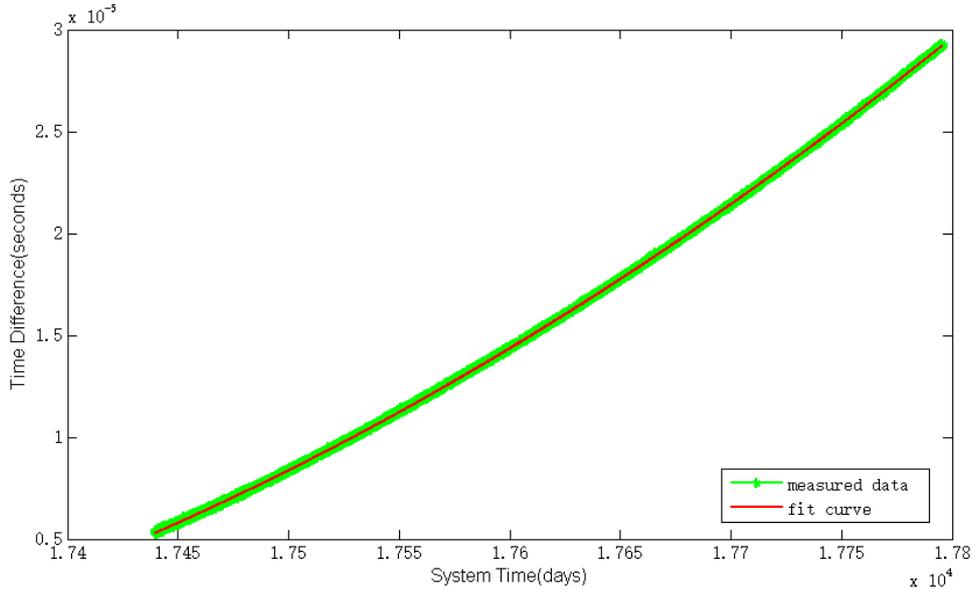
Fig. 3 Hydrogen maser long-term drift curve fitting. The *red solid line* corresponds to the fitting of the GPS and hydrogen maser 1PPS clock difference curve (the *thick green dotted line*, which corresponds to the *yellow line* in Fig. 2). The x-axis is the unix system time (unit in days) starting from 1970.01.01. The unit of the y-axis is sec.
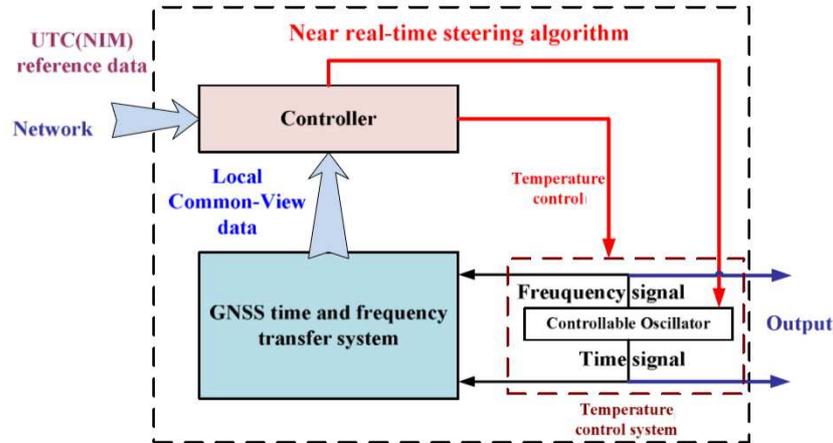
Fig. 4 NIMDO design principle. The core component of NIMDO is a low-cost rubidium oscillator controlled by UTC (NIM) in near real time, which was built at the National Institute Metrology (NIM), China. Through the use of NIMDO, the time and frequency standards can be traced to UTC (NIM) directly with an accuracy of $5\,\mathrm{ns}$.

to adjustment in operations, it will take a few months for the maser to recover to the stable state. Another method to adjust the output frequency of the hydrogen maser without affecting its working state is to use an external Auxiliary Output Generator (AOG), which is able to fine tune the external reference frequency at the relative level of 1×10^{-19}.

3.2 Time Delay Measurement

The time delays of different signal paths were measured using Keysight 53230A frequency counters in time interval mode. To measure the time delay, a pulse signal was

generated and split into two channels, one of which was sent to channel A of the counter directly, and the other sent to the cable being measured and looped back to channel B of the counter. Then the signal delay of the two channels was measured, which represents the cable delay.

By this method, the time delay of the signal from the focus cabin to the backend room was measured, which is $D_{\mathrm{focus}} = 19.93\,\mu\mathrm{s} \pm 0.4\,\mathrm{ns}$. The total measurement uncertainty comes from random uncertainty, time-based uncertainty and systematic uncertainty. The standard deviation of the measurement is $44\,\mathrm{ps}$, so the random uncertainty

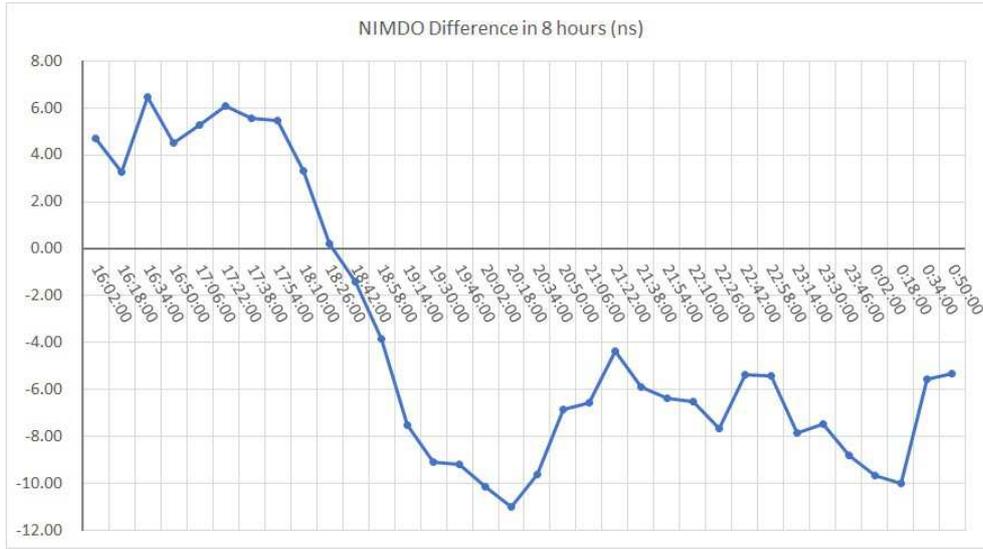**Fig. 5** NIMDO difference with respect to UTC-NIM in 8 hr of 2018.11.14 at FAST (ns).
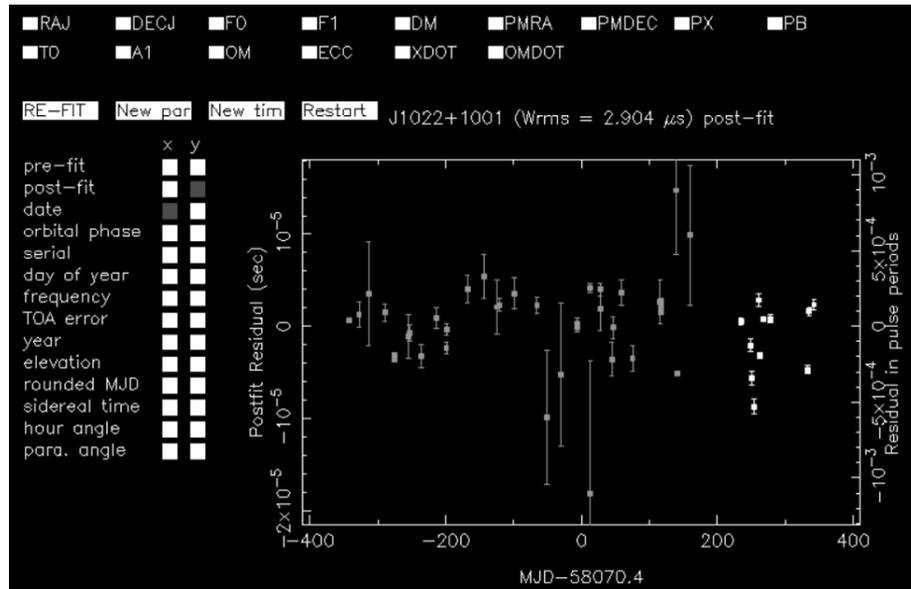

Fig. 6 Pulsar timing residuals of FAST and the Parkes telescope by Nov 2018.

of the 95% confidence range is $88\,\mathrm{ps}$. The evaluated time-based uncertainty of the counter is $32\,\mathrm{ps}$ and the evaluated systematic uncertainty is $260\,\mathrm{ps}$. As a whole, the total uncertainty of the delay measurement is $\epsilon_{\mathrm{focus}} = \pm0.3\,\mathrm{ns}$.

The time delay of the GPS signal in the co-axial cable from the antenna to the time server was measured in the same way, which is $D_{\mathrm{gps}} = 71.2\,\mathrm{ns} \pm 0.5\,\mathrm{ns}$.

The computer time of the receiver system is NTP time from GPS time servers. The NTP time offset is measured by the ntpd and chronyc tools, which is less than $5\,\mathrm{ms}$ in the local network.

3.3 NIMDO Standard

An improvement in the time and frequency standard system is the NIMDO time frequency source. NIMDO is a realization of Real Time Remote Calibration (RTRC, Liang et al. 2013; Lombardi 2010) utilized in the field of time frequency metrology, which aims to develop an easy and fast way for clients to calibrate the time and frequency standards by comparing to UTC-NIM (National Time and Frequency Primary Standard of China) in near real time.

Figure 4 shows the flowchart of NIMDO. NIMDO traces the Global Navigation Satellite System (GNSS) Common-View (CV) data from reference stations and the
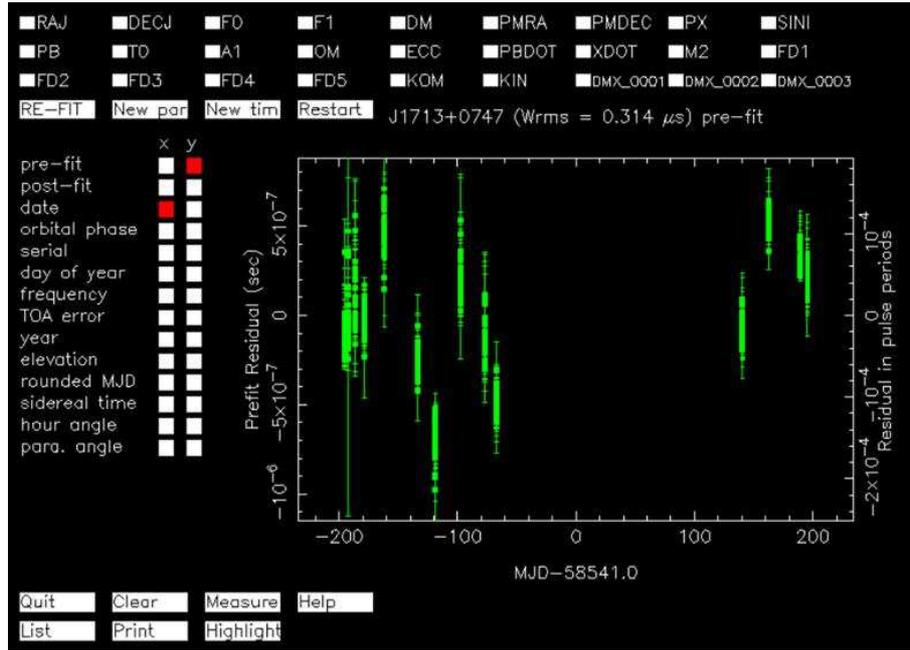
Fig. 7 Pulsar J1713+0747 timing residuals from FAST by Sep 2019.

local station through near real time communication. After computing, the time and frequency differences between different stations are retrieved. By connecting NIMDO and AOG through a serial port, the output frequency of AOG can be fine tuned by NIMDO according to the real time UTC-NIM, comparing and averaging the result. The time and frequency stability of NIMDO is respectively better than $5\,\mathrm{ns}$ and 6×10^{-13} when averaging over one day.

Figure 5 is the NIMDO time difference compared to UTC-NIM at the FAST site. Within a total of 8 hr from 16:02 to 0:50, the NIMDO difference towards UTC-NIM is less than $\pm 11\,\mathrm{ns}$. The standard deviation of the time difference series is $5.71\,\mathrm{ns}$ and the average difference is $-3.73\,\mathrm{ns}$.

4 PULSAR TIMING OBSERVATION

In this part, we discuss the ongoing FAST pulsar timing observation. Pulsar timing observations at FAST started in April 2018, right after the discovery of the millisecond pulsar J0318+02 by a joint search program involving *Fermi*-LAT and FAST (Backer et al. 1982). Pulsars J1022+1001 and J1713+0747 were chosen for timing observations. The digitized signals were channelized and quickly integrated over several microseconds by the pulsar spectrometer attached to the Collaboration for Astronomy Signal Processing and Electronics Research (CASPER) ROACH2 hardware facility. The integrated spectrum is transported to the storage server through $10\,\mathrm{GB}$ ethernet ports and saved in PSRFITS files, and then analyzed by pulsar timing routine Tempo2 (Hobbs et al. 2006). The Times of Arrival (ToAs) of pulsars are fitted with timing models incorporating the pulsar spin, dispersion measure (DM) and orbital parameters, and the post-fit timing residuals are obtained. Figure 6 displays the timing residuals from FAST timing observations of pulsar J1022+1001 in a period of half a year, compared with residuals from the Parkes telescope in Australia.

Altogether, 23 timing observations were carried out over 6 months, and every single timing observation lasted for 30 minutes. The gray dots in Figure 6 represent the post-fit timing residuals from the Parkes telescope, while the white dots signify the post-fit timing residuals from FAST. The weighted RMS of post-fit timing residuals is less than $3.0\,\mathrm{\mu s}$. As a method of improvement to further reduce the pulsar timing residuals, more detailed polarization calibrations of the telescope need to be performed.

After polarization calibrations were carried out, the result of timing observation of pulsar J1713+0747 by Sep 2019 was further improved compared to the earlier result, as demonstrated in Figure 7.

5 SUMMARY

We have described the time and frequency standard system for FAST receivers, including the hydrogen maser, GPS time servers, and AOG and NIMDO time frequency sources. The system frequency stability reaches the level

of $8 \times 10^{-14}\,\mathrm{d}^{-1}$ and the time accuracy and stability reach the level of $< 5\,\mathrm{ns}$. Recent pulsar timing observations at FAST indicate that the accuracy and stability of the time frequency standards meet the requirements of pulsar timing observations.

References

Rogers, A. E. E., & Moran, J. M. 1981, IEEE Transactions on Instrumentation and Measurement, IM-30, 283

Thompson, A. R., & Moran, J. M. 1989, Interferometry and Synthesis in Radio Astronomy (WILEY-VCH), 340

Backer, D. C., Kulkarni, S. R., Heiles, C., et al. 1982, Nature, 300, 615

Li, D., & Pan, Z.-C. 2016, Radio Science, 51, 1060

Hobbs, G. B., Edwards, R. T., & Manchester, R. N. 2006, MNRAS, 369, 655

Liang, K., Zou, F., Chao, P., et al. 2013, in Proceedings of IFCS-EFTF2013, Real-Time Remote Calibration (RTRC) System for Time and Frequency,

Lombardi, M. A. 2010, in Proc. of 2010 NCSL International Workshop and Symposium, A NIST Disciplined Oscillator

Nan, R. D., et al. 2011, International Journal of Modern Physics D, 20, 989

Riley, W. J. 2008, Handbook of Frequency Stability Analysis